Corridor Navigation with a LiDAR/INS Kalman Filter Solution

William Travis*, Adam T. Simmons**, and David M. Bevly***
Auburn University, 200 Broun Hall, Auburn, AL 36849, U.S.A.

***Abstract*— Autonomous capability requires reliable and robust navigation solutions in multiple environments. GPS has become an effective tool but is not suitable for all environments. Laser scanners are quickly making their presence known in the navigation field and are proven to have a variety of uses. This paper investigates the use of LiDAR within an indoor corridor environment (i.e. hallway) to update IMU measurements.**

The LiDAR is combined with an IMU in a Kalman filter to produce estimates of vehicle velocity, heading, lateral error, and sensor biases. It is shown how this combination is effective in providing accurate state estimates while removing sensor errors due to noise and bias.

I. Introduction

The popularity of autonomous ground vehicles, or AGVs, is quickly increasing with the advent of better and more reliable navigation technologies. There is a large niche for such a vehicle, ranging from agricultural machines, to civilian and military transportation, to unmanned combat machines, to search and rescue vehicles, and so on. Filling this current void requires the improvement in robustness in current technologies, as well as developing new methods to adequately and safely navigate through many environments and over varying terrains.

Inertial measurement units (IMUs) are often the basis of a navigation system. They provide multiple degree of freedom measurements at fast update rates to capture higher dynamics. IMU affordability has greatly improved over the past few years with the development of silicon based sensors and micro-electromechanical sensing (MEMS) devices. Of course, accuracy often improves with cost, which reduces the feasibility of some applications. The negative aspect of IMUs, especially low cost versions, is that they are the handicap in navigation and control systems. Such systems require clean, unbiased measurements, which are not provided by off the shelf IMUs. Typically, a simple filter can alleviate the problems due to noise, but sensor biases change with respect to temperature, environment, and time, and are harder to determine.

Kalman filtering is commonly used to reduce sensor errors and develop a navigation solution. A Kalman filter is a type of high-level filter that minimizes a cost function to provide accurate state estimates of a system. AGVs usually rely on a navigation solution comprised of GPS and inertial measurements. Coupling the output of the two measurement devices uses the good qualities of one sensor to overcome the downfall of the other. Contrary to an IMU, GPS offers unbiased measurements with high precision (depending on the receiver quality) but slow update rates. Where IMUs normally output in the 50Hz to 100Hz range, GPS outputs only in the 1Hz to 5Hz range. The Kalman filter uses the GPS measurements to correct the navigation errors created by the IMU. This has been a proven approach to obtain accurate system states, which leads to a high-quality navigation solution [2], [4].

Satellites are not always in direct view of the GPS receiver, which is hindering the development of reliable AGVs. Environmental constraints can either completely block the signal, or degrade the signal to the point where it is of no use. Jamming is a similar issue in combat environments, where the opposition can cheaply and effectively knock out the GPS signals or broadcast incorrect messages. If the GPS signal is suddenly lost, jammed, or known to be incorrect, some critical system states become unobservable without additional sensors. The navigation solution is forced to integrate noisy, biased IMU measurements, affecting positioning accuracy and control ability.

The focus of this research is to investigate navigation without the use of GPS. A light detection and ranging device (LiDAR) is used in conjunction with data from a MEMS based IMU to formulate a suitable navigation solution. LiDAR is has been used as a navigation tool on both aerial [3] and ground vehicles [5], [7]. Specifically, this paper examines the operation of a ground vehicle in an indoor corridor environment. The lack of GPS updates is compensated by the use of a LiDAR. The LiDAR updates the following critical vehicle states: heading, velocity, and lateral error. This type of navigation would bode well in many environments, such as an urban canyon, forest, indoor corridor, or in jammed environments.

II. Testing Apparatus

A. Experiment

A cart was outfitted with an IMU and LiDAR. Details of the sensors are provided in the ensuing sections. The cart had four independent wheels that were free to rotate about the X and Z axes of a vehicle coordinate frame (X being forward, Z being down). It was manually pushed down a corridor at different velocities while data was logged from the IMU and LiDAR. The absence of an engine or motor to translate the cart reduced the amount of vibration that the sensitive IMU would pick up. The majority of the noise stemmed from a fan

* e-mail: traviwe@auburn.edu
** e-mail: simmoat@auburn.edu, IEEE Student Member
*** e-mail: dmbevly@auburn.edu

on a power supply and irregularities along the ground as the cart rolled over it. Data from each run was passed through a Kalman filter post process to develop an estimation of velocity, heading, and lateral error.

B. IMU

The IMU used in this analysis was a Crossbow IMU400CC-100, capable of providing 3 axis accelerations and rotations. The sensors in the unit are MEMS based, and have inherent walking biases and scale factor errors. The Crossbow output is recorded at 100Hz. Two scenarios are covered in this paper and require two different input matrices. The first input set contains longitudinal acceleration and yaw rate, and the second input set adds lateral acceleration.

$$u_1 = \begin{bmatrix} \ddot{x} \\ \dot{\psi} \end{bmatrix} \quad u_2 = \begin{bmatrix} \ddot{a_x} \\ \dot{\psi} \\ \ddot{a_y} \end{bmatrix} \tag{1}$$

C. LiDAR

LiDAR is used to "visually" access the environment and extract information, which is used to update the IMU data. The SICK LMS 221 LiDAR projects infrared laser pulses into the local environment and records their "time of flight" and reflected intensity at 180 scanning points over the range 0° to 180° at a rate of $13.32\ ms$ per scan. The scanning points and the associated distances give a 2D image of the environment, a polar coordinate position and distance, at each time step (θ_k, d_{θ_k}). Using these measurements, a local heading ψ, velocity, and lateral position y_{lat} are found. The measurement matrix is as follows:

$$y = \begin{bmatrix} \dot{x_m} \\ \psi_m \\ y_{lat_m} \end{bmatrix} \tag{2}$$

The LiDAR's heading estimate ψ_m is found as a function of the center of the hallway. A hallway's center can be estimated by halving the distance between the corners of the hallway. Each corner in a hallway has the unique distinction of an edge, or the change in distance for a given set of data points (θ, d_θ) and $(\theta + \delta\theta, d_{\theta+\delta\theta})$ located at a corner is large (Figure 1). These corners are determined as spikes in the scanning points derivative. Once the center of the hallway is determined, the ψ_m estimate is determined as the angle between the 90^o center-line of the LiDAR and the center of the hallway (Figure 2). Finally, the lateral position of the LiDAR is found as a distance from the hallway's center. Two distances $d_{\bar{\theta},i}$ are determined at $\bar{\theta} = \pm 60^o$ angles from the center of the hallway. These distance are used to determine the lateral distance from the LiDAR to the edge of the wall $y_{lat,i}$.

$$y_{lat,1} = d_{\bar{\theta},1} \cos(90^o - \bar{\theta}) \tag{3}$$

$$y_{lat,2} = d_{\bar{\theta},2} \cos(90^o - \bar{\theta}) \tag{4}$$

Given the lateral distances from the LiDAR to the edge of the wall, the lateral position of the LiDAR from the center of the hall is given as

$$y_{lat} = y_{lat,1} - y_{lat,2} \tag{5}$$

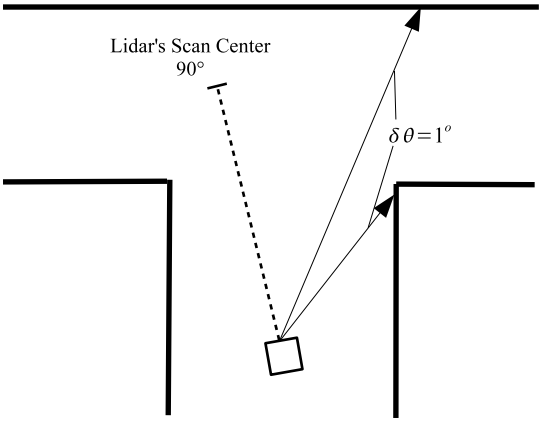

Fig. 1. Corner detection using Lidar

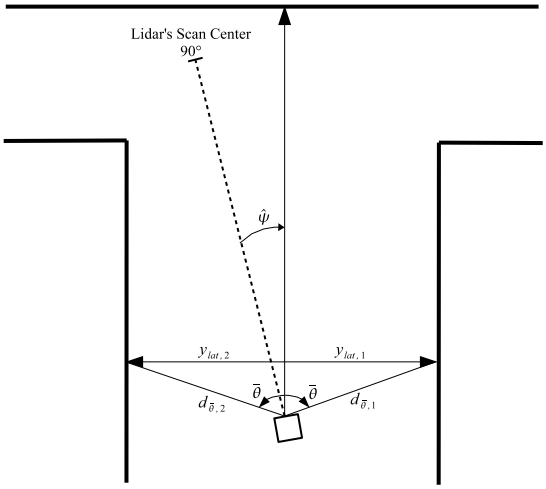

Fig. 2. ψ and lateral position y measurements

All of the LiDAR's data was run through a 10 point moving average filter to minimize the effect of any blips that occurred. The tests were run in a fairly controlled environment with smooth corridors, minus occasional doorways and small, miscellaneous objects. Other types of corridors, such as rows of trees lining a road, will be less consistent and generate more data blips. The moving average filter aids in smoothing out the corridors and provides the Kalman filter a more discernible measurement.

III. Navigation with State Estimation

A. System Model

To thoroughly investigate the capabilities of utilizing LiDAR for vehicle navigation, two kinematic models were derived. The first mathematical analysis assumes zero vehicle sideslip, so the discrepancy between vehicle heading and course is due only to error and not to a lateral velocity. The following five states are estimated: velocity, longitudinal accelerometer bias, heading, yaw gyro bias, and lateral error. Inputs to the system from the IMU are stated in u_1 of equation 1 and measurements are provided by the LiDAR as shown in equation 2. Note that the $\dot{x}$ component for lateral error, y_{lat}, is

a lateral velocity in the environmental coordinate frame, not the vehicle coordinate frame. There is zero lateral velocity in the vehicle coordinate system due to the zero sideslip assumption.

$$\dot{x} = \begin{bmatrix} \ddot{x} - b_a \\ \dot{b}_a \\ \dot{\psi} - b_r \\ \dot{b}_r \\ \dot{x}\sin\psi \end{bmatrix} \quad x = \begin{bmatrix} \dot{x} \\ b_a \\ \psi \\ b_r \\ y_{lat} \end{bmatrix} \tag{6}$$

The state space realizations to fill in the typical $\dot{x} = Ax + Bu, y = Cx + Du$ format are as follows [1]:

$$A = \begin{bmatrix} 0 & -1 & 0 & 0 & 0 \\ 0 & 0 & 0 & 0 & 0 \\ 0 & 0 & 0 & -1 & 0 \\ 0 & 0 & 0 & 0 & 0 \\ \sin\psi & 0 & \dot{x}\cos\psi & 0 & 0 \end{bmatrix} \tag{7}$$

$$B = \begin{bmatrix} 1 & 0 \\ 0 & 0 \\ 0 & 1 \\ 0 & 0 \\ 0 & 0 \end{bmatrix} \quad C = \begin{bmatrix} 1 & 0 & 0 & 0 & 0 \\ 0 & 0 & 1 & 0 & 0 \\ 0 & 0 & 0 & 0 & 1 \end{bmatrix}$$

In some instances, the sideslip can be used as an analysis tool or as a focal point of control and merits further investigation. The second kinematic model acknowledges that the vehicle can translate laterally within its own coordinate frame, creating an additional lateral acceleration component. It uses the same measurements from the LiDAR but couples them with the inputs from u_2 in equation 1. The sixth estimated state is lateral velocity in the vehicle frame.

$$\dot{x} = \begin{bmatrix} \ddot{x} - b_a \\ \dot{b}_a \\ \dot{\psi} - b_r \\ \dot{b}_r \\ \dot{x}\sin\psi + \dot{V}_y\cos\psi \\ \dot{V}_y \end{bmatrix} \quad x = \begin{bmatrix} \dot{x} \\ b_a \\ \psi \\ b_r \\ y_{lat} \\ V_y \end{bmatrix} \tag{8}$$

$$A = \begin{bmatrix} 0 & -1 & 0 & 0 & 0 & 0 \\ 0 & 0 & 0 & 0 & 0 & 0 \\ 0 & 0 & 0 & -1 & 0 & 0 \\ 0 & 0 & 0 & 0 & 0 & 0 \\ \sin\psi & 0 & \dot{x}\cos\psi & 0 & 0 & \cos\psi \\ 0 & 0 & 0 & 0 & 0 & 0 \end{bmatrix} \tag{9}$$

$$B = \begin{bmatrix} 1 & 0 & 0 \\ 0 & 0 & 0 \\ 0 & 1 & 0 \\ 0 & 0 & 0 \\ 0 & 0 & 0 \\ 0 & 0 & 1 \end{bmatrix} C = \begin{bmatrix} 1 & 0 & 0 & 0 & 0 & 0 \\ 0 & 0 & 1 & 0 & 0 & 0 \\ 0 & 0 & 0 & 0 & 1 & 0 \end{bmatrix}$$

[1]The direct transmission matrix is zero

B. Noise Statistics

Noise statistics for the inputs were obtained by recording static data and finding the mean and variance of each measurement. Biases are assumed to be constant in the system model, but the Kalman filter was told that they could vary slightly over time. This is a preventive measure to effectively deter the Kalman filter from "going to sleep" and holding the bias states constant when they can change in reality. Total lateral movement is a function of $\dot{x}$, ψ, and a_y. In the first scenario neglecting sideslip, the standard deviation in the lateral error is already accounted for in the $\dot{x}$ and ψ terms. In theory, $\sigma_{y_{lat}}$ should be set to zero to refrain from injecting unnecessary process noise into the system. This parameter essentially can become a tuning knob to attempt to estimate unmodeled disturbances. This parameter is non Gaussian in relation to the other statistics which technically makes the Kalman filter not optimal, but the effects are minimal in many situations (including the one investigated). In the second scenario, $\dot{x}$ and ψ again account for some process noise in y_{lat}, but there is additional process noise due to the lateral acceleration measurement that must be implemented into the system. As it turns out, accounting for the process noise when estimating V_y automatically injects the process noise into the lateral error state so the term remains zero. Together, these statistics form the continuous process covariance matrix in equation 10 [2]. The Q shown is for scenario two. The Q for scenario one is identical except it does not have the last row and column.

$$Q_2 = \begin{bmatrix} \sigma_{a_x} & 0 & 0 & 0 & 0 & 0 \\ 0 & a_{walk} & 0 & 0 & 0 & 0 \\ 0 & 0 & \sigma_r & 0 & 0 & 0 \\ 0 & 0 & 0 & r_{walk} & 0 & 0 \\ 0 & 0 & 0 & 0 & \sigma_{y_{lat}} & 0 \\ 0 & 0 & 0 & 0 & 0 & \sigma_{a_y} \end{bmatrix} \tag{10}$$

Measurement noise statistics were calculated by averaging multiple static data sets taken along the testing path. The following discrete measurement covariance matrix is produced:

$$R = \begin{bmatrix} \sigma_{\dot{V}}^2 & 0 & 0 \\ 0 & \sigma_{\dot{\psi}}^2 & 0 \\ 0 & 0 & \sigma_{y_{lat}}^2 \end{bmatrix} \tag{11}$$

For LiDAR, the noise is sufficiently estimated by examining a static, or stationary, set of data. For this paper, the author assumes a sufficient gauge of noise, by taking into account the static data sets at the beginning, middle, and end of the hall. For a more thorough examination of the noise, techniques in Detection and Estimation could be used to determine more appropriate noise characteristics [1].

C. Kalman Filter

An extended Kalman filter was chosen due to the nonlinearities in the system model. Specifically, the filter used is a continuous-discrete hybrid filter known as an extended Kalman-Bucy filter. This is a preferred method when dealing

[2]Actual values for Q and R are found in the appendix

with sampled data measurements of a continuous process. This specific method and following equations are outlined in more detail in [6].

State Estimate Propagation

$$\hat{x}(t_k^-) = \hat{x}(t_{k-1}^+) + \int_{t_{k-1}}^{t_k} f[\hat{x}(\tau^-), u(\tau), \tau]d\tau \quad (12)$$

Covariance Estimate Propagation

$$P(t_k^-) = P(t_{k-1}^+) + \int_{t_{k-1}}^{t_k} [A(\tau)P(\tau) + P(\tau)A(\tau)^T + B_w(\tau)Q(\tau)B_w(\tau)^T]d\tau \quad (13)$$

Kalman Filter Gain Calculation

$$L(t_k) = P(t_k^-)C(t_k)^T[C(t_k)P(t_k^-)C(t_k)^T + R(t_k)]^{-1} \quad (14)$$

State Estimate Update

$$\hat{x}(t_k^+) = \hat{x}(t_k^-) + L(t_k)[y(t_k) - C(t_k) * \hat{x}(t_k^-)] \quad (15)$$

Covariance Estimate Update

$$P(t_k^+) = [I - L(t_k)C(t_k)]P(t_k^-) \quad (16)$$

IV. Results

A. Scenario 1A

As stated earlier, scenario one investigates the use of LiDAR in vehicle navigation when the vehicle's lateral velocity component is assumed to be zero.

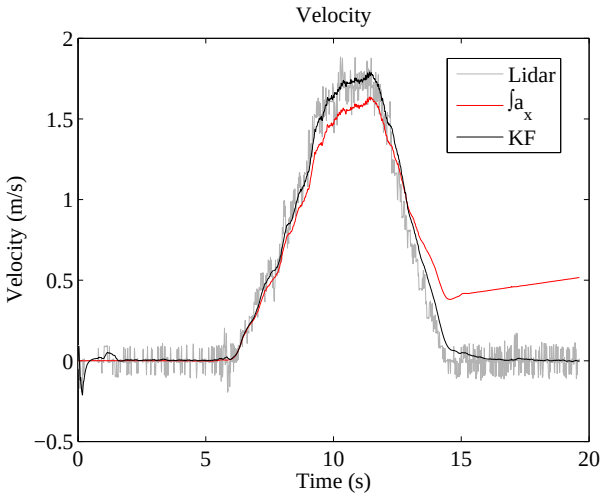

Fig. 3. Velocity assuming $\beta = 0$ and $\sigma_{y_{lat}}$=0

The LiDAR does a more than adequate job of estimating the vehicle states. The estimates of velocity (Figure 3) and heading (Figure 4) capture the high dynamics as measured by the IMU during short durations, but they follow the LiDAR measurements long term to remove the effect of biases in the system. The biases are well represented as they slowly drift to a constant value (Figure 6). Lateral error in Figure 5 quickly tracks an initial offset of 0.25 meters, but is slow to respond to other lateral changes.

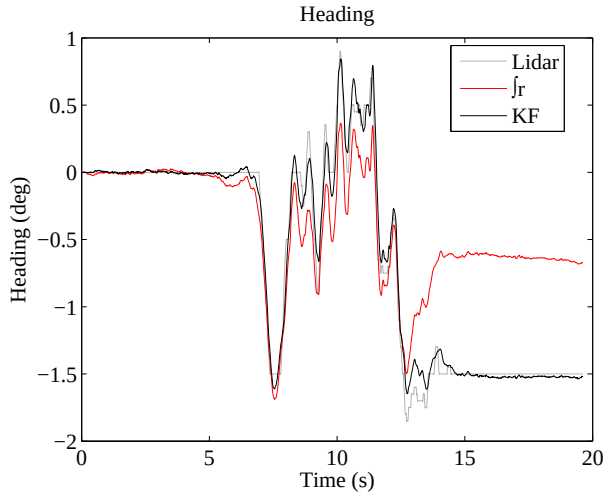

Fig. 4. ψ assuming $\beta = 0$ and $\sigma_{y_{lat}}$=0

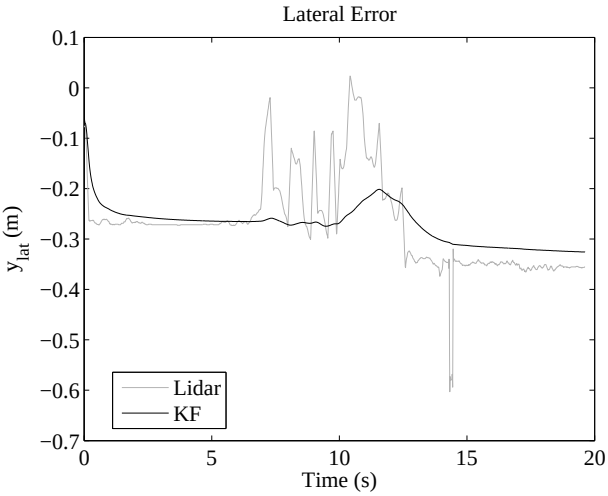

Fig. 5. Lateral error assuming $\beta = 0$ and $\sigma_{y_{lat}}$=0

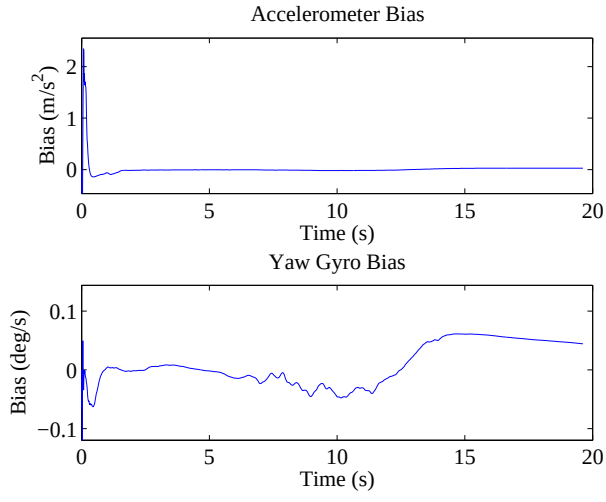

Fig. 6. Bias estimates assuming $\beta = 0$ and $\sigma_{y_{lat}}$=0

B. Scenario 1B

To investigate the slow tracking of the lateral error estimation, the $\sigma_{y_{lat}}$ "knob" was tweaked to account for unmodeled disturbances or dynamics in the system. Discrete values of 0.01 and 0.1 meters were inserted into the Q matrix. This value has minimal affect on the velocity, heading, and bias estimates, but it has an obvious affect on the lateral error estimate. As the value approaches zero, the estimate is filtered more. As it moves away from zero, the estimate converges on the LiDAR measurement. This effect is shown in the following figures 7 and 8.

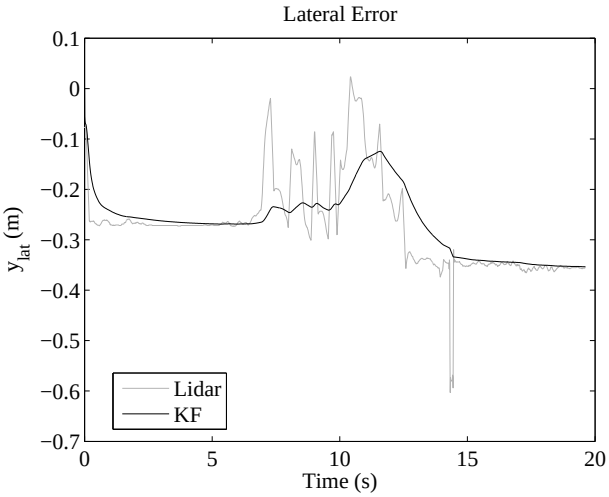

Fig. 7. Lateral error assuming $\beta = 0$ and $\sigma_{y_{lat}}$=0.01

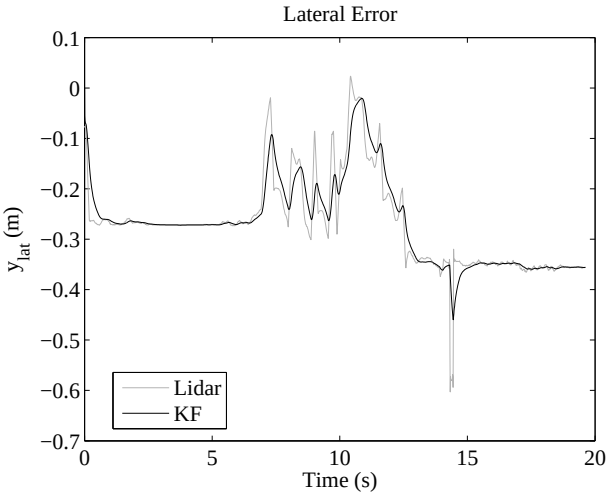

Fig. 8. Bias estimates assuming $\beta = 0$ and $\sigma_{y_{lat}}$=0.1

C. Scenario 2

The second scenario investigated the effectiveness of navigation with LiDAR when a lateral acceleration measurement is available. Often this measurement is corrupted by the system or there are no suitable measurements to make its derivative observable. The test bed did not contain many additional sources of error so the lateral accelerometer recorded fairly clean data. There was no lateral velocity sensor on board which made lateral velocity and lateral accelerometer bias unobservable. Bias was removed post process and assumed to be constant. This is a safe assumption because of the short duration of each test.

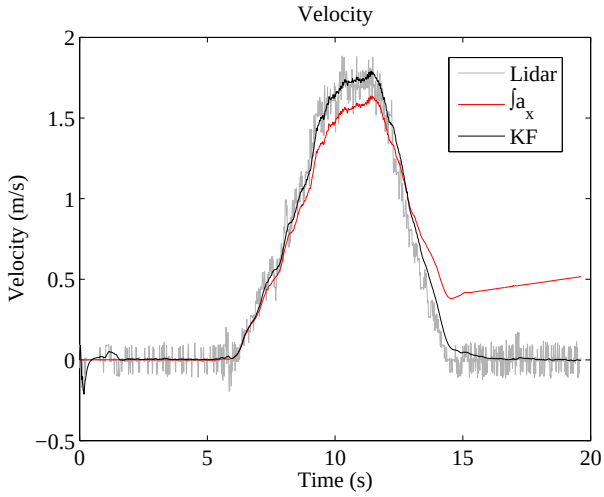

Fig. 9. Velocity assuming $\beta \neq 0$ and $\sigma_{y_{lat}}$=0

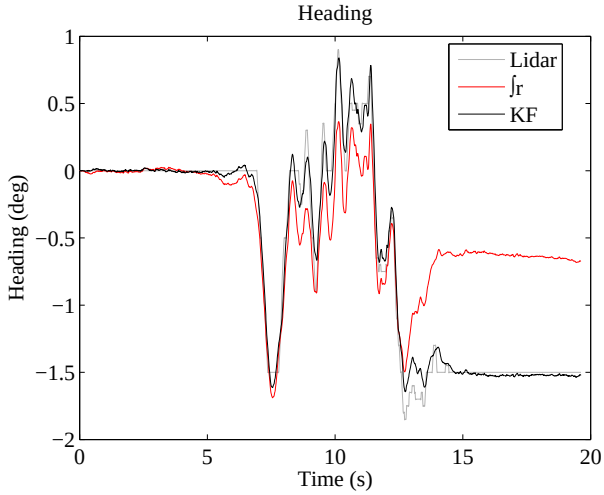

Fig. 10. ψ assuming $\beta \neq 0$ and $\sigma_{y_{lat}}$=0

The additional input has minimal affect on the velocity (Figure 9) and heading (10) states, but the lateral error estimate (Figure 11) uses it to provide a cleaner solution.

V. Conclusions

A LiDAR/INS solution has been shown to provide accurate state estimates for a vehicle in a corridor environment. The reliable measurements and statistical properties of the LiDAR form a suitable companion for an IMU when using a Kalman filter to calculate a solution. Inertial errors due to integration of noise and bias are removed, and the estimates still track the higher system dynamics of the vehicle. A proposed method of tuning the performance of the Kalman filter has been offered by means of varying a process noise statistic on lateral velocity

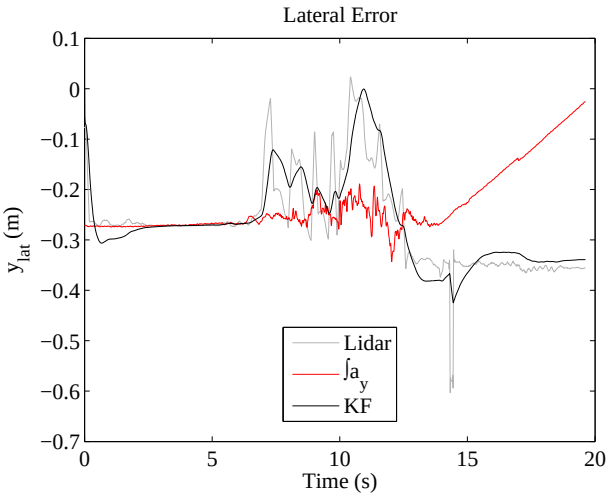

Fig. 11. Lateral error assuming $\beta \neq 0$ and $\sigma_{y_{lat}}$=0

to account for unmodeled dynamics and/or disturbances to the system.

VI. Future Research

This preliminary study of LiDAR as a navigation aid has provided a foundation for more extensive research. The next step is to try similar tests in different environments. The LiDAR and IMU will be instrumented on a 4 wheeler to be entered into the 2005 DARPA Grand Challenge and driven on off road courses. Corridors will consist of road edges or tree lines and GPS will be used as a truth measurement. Navigation solutions will be determined post process to evaluate their reliability, and then they will be implemented on the vehicle and run in real time. A throttle and steering controller will use the outputs of the Kalman filter to navigate the vehicle without the use of GPS.

VII. Appendix

$\sigma_{a_x} = 0.032068 \quad m/s^2$
$a_{walk} = 9.81e-9 \quad m/s^2$
$\sigma_r = 8.5464e-6 rad/s$
$r_{walk} = 1.7453e-11 \quad rad/s$
$\sigma_{y_{lat}} = 0, 0.01, 0.1 \quad m$
$\sigma_{a_y} = 0.053432 \quad m/s^2$
$\sigma_V = 0.028 \quad m/s$
$\sigma_\psi = 0.001 \quad rad$
$\sigma_{y_{lat}} = 0.02 \quad m$

VIII. Acknowledgments

The authors wish to acknowledge SciAutonics for providing the use of a SICK LMS 221 LiDAR, and Rob Daily for his helpful insight.

References

[1] Martin D. Adams. Lidar design, use, and calibration concepts for correct environmental detection. *IEEE Transactions on Robotics and Automation*, 16(6):753–761, December 2000.

[2] David M. Bevly. Global positioning system (gps): A low cost velocity sensor for correcting inertial sensor errors on ground vehicles. *Journal of Dynamic Systems, Measurement, and Control*, 126:1–10, June 2004.

[3] Jacob Campbell, Maarten Uijt de Haag, and Frank van Graas. Light detection and ranging-based terrain navigation - a concept exploration. *Institute of Navigation GPS/GNSS*, September 2003.

[4] Gamini Dissanayake, Salah Sukkarieh, Eduardo Nebot, and Hugh Durrant-Whyte. The aiding of a low-cost strapdown inertial measurement unit using vehicle model constraints for land vehicle applications. *IEEE Transactions on Robotics and Automation*, 17(5):731–747, October 2001.

[5] Rui Hirokawa, Kenji Nakakuki, Koichi Sato, and Ryuichi Ishihara. Threading the maze: Gps/ins, landmark sensing, and obstacle avoidance. *GPS World*, 15(11):20–26, November 2004.

[6] Robert F. Stengel. *Optimal Control and Estimation*. Dover Publications, Inc., 31 East 2nd Street, Mineola, NY 11501, first edition, 1994.

[7] J. Talaya, R. Alamus, E. Bosch, A. Serra, W. Kornus, and A. Baron. Integration of a terrestrial laser scanner with gps/imu orientation sensors. *International Society for Photogrammetry and Remote Sensing*, XXXV:19–24, July 2004.